

RESEARCH LETTER

10.1029/2018GL078281

Key Points:

- Midsummer Arctic sea ice extent anomalies seemingly lead to significant predictive skill for high-latitude climate up to 3 months in advance
- Midsummer Arctic sea ice anomalies are linked to polar temperature throughout the troposphere into September and at the surface into October
- The results are reproducible in observations, in output from the CMIP5 archive, and in prediction experiments from the APPOSITE project

Supporting Information:

- Supporting Information S1

Correspondence to:

S. He,
shengping.he@uib.no

Citation:

He, S., Knudsen, E. M., Thompson, D. W. J., & Furevik, T. (2018). Evidence for predictive skill of high-latitude climate due to midsummer sea ice extent anomalies. *Geophysical Research Letters*, 45, 9114–9122. <https://doi.org/10.1029/2018GL078281>

Received 9 APR 2018

Accepted 27 JUL 2018

Accepted article online 2 AUG 2018

Published online 2 SEP 2018

©2018. American Geophysical Union.
All Rights Reserved.

Evidence for Predictive Skill of High-Latitude Climate Due to Midsummer Sea Ice Extent Anomalies

Shengping He^{1,2} , Erlend M. Knudsen³ , David W. J. Thompson⁴, and Tore Furevik^{1,2}

¹Geophysical Institute, Bjerknes Centre for Climate Research, University of Bergen, Bergen, Norway, ²Bjerknes Centre for Climate Research, Bergen, Norway, ³Institute for Geophysics and Meteorology, University of Cologne, Albertus-Magnus-Platz, Cologne, Germany, ⁴Department of Atmospheric Science, Colorado State University, Fort Collins, CO, USA

Abstract Previous work has explored the linkages between Arctic sea ice extent (SIE) anomalies at the end of the summer melt season and high-latitude climate. Here we show that Arctic midsummer SIE anomalies provide predictive skill on time scales of ~2–3 months for high-latitude climate. Midsummers characterized by low SIE are associated with significant positive temperature and easterly wind anomalies throughout the high-latitude troposphere through September and significant positive temperature anomalies at the Arctic surface into October. The inferred predictive skill for autumn climate derives from the persistence of the sea ice field. It is robust throughout the Arctic basin and is supported in climate models from the fifth phase of the Coupled Model Intercomparison Project archive and in prediction experiments from the Arctic Predictability and Prediction on Seasonal to Interannual Time scales project. It is theorized that the predictive skill derives from (1) the anomalous storage of heat in the Arctic Ocean during periods of low summertime SIE and (2) the delayed formation of sea ice during the following autumn months.

Plain Language Summary Here we analyze the evidence for predictability of high-latitude climate that derives from Arctic sea ice extent (SIE) anomalies. We demonstrate that the continuous observed lagged correlations between Arctic sea ice anomalies and Arctic/high-latitude climate are most robust in association with midsummer (July) SIE. The linkages between midsummer SIE anomalies and Arctic/high-latitude climate are significant well into autumn and have potential implications for the prediction of high-latitude climate up to 3 months in advance. The results have implications for the influence of long-term decreases in summertime sea ice on climate change over the high latitudes.

1. Introduction

Arctic sea ice extent (SIE) is frequently defined as the total area of the Arctic Ocean that is covered by at least 15% floating ice, climatologically (1981–2010) ranging from a maximum value of 15.60×10^6 km² in March to a minimum value of 6.54×10^6 km² in September (Fetterer et al., 2017). Satellite observations reveal significant declines in Arctic SIE over the past few decades in all seasons, with the largest decreases found at the end of the summer melt season. The trends in September SIE were $-8.6 \pm 2.9\%$ per decade over the period 1979–2006 (e.g., Serreze et al., 2007; Stroeve et al., 2007) and increased to $-13.0 \pm 2.4\%$ per decade over the period 1979–2017 (Fetterer et al., 2017), indicating an accelerated reduction of SIE over the past decade.

Arctic sea ice covers a relatively small fraction of the globe, but it nevertheless exerts a substantial impact on the climate system due to its important role in reflecting solar radiation and blocking the direct exchange of latent and sensible energy between the atmosphere and the underlying ocean (e.g., Budyko, 1969; Frankignoul et al., 2014; Gao et al., 2015; Maykut, 1982; Orsolini et al., 2012; Petrie et al., 2015; Serreze & Barry, 2011). Hence, considerable effort has been devoted to exploring the inherent predictability of Arctic sea ice and its potential role on midlatitude weather.

The inherent predictability of Arctic sea ice has been a research focus for decades (e.g., Barnett, 1980; Blanchard-Wrigglesworth, Armour, et al., 2011; Blanchard-Wrigglesworth, Bitz, Holland, 2011; Chevallier et al., 2013; Day et al., 2014; Drobot, 2007; Holland et al., 2011; Lindsay et al., 2008; Rigor & Wallace, 2004; Sigmond et al., 2013; Stroeve et al., 2016; Walsh, 1980; Walsh & Johnson, 1979; Wang et al., 2013). In general, predictability of SIE emerges on three different time scales: (1) time scales of ~2–4 months due to the relatively slow exponential decay of sea ice anomalies; (2) time scales of seasons due to the storage of sea ice anomalies in the underlying sea surface temperature field (i.e., the *reemergence* of sea ice anomalies;

Blanchard-Wrigglesworth, Armour, et al., 2011); and (3) time scales of decades due to anthropogenic climate change (i.e., sea ice will continue to melt as the globe warms; Kirtma et al., 2013) and due to low-frequency variability in poleward ocean heat transport (Årthun et al., 2017; Yeager et al., 2015).

The potential influence of Arctic sea ice anomalies on the atmosphere has also been a research focus for decades (e.g., Alexander et al., 2004; Bhatt et al., 2008; Blüthgen et al., 2012; Cvijanovic et al., 2017; Deser et al., 2004, 2010; Herman & Johnson, 1978; Screen et al., 2013, 2014). But interest in the potential impacts of Arctic sea ice on climate has grown exponentially in recent years due to a series of studies that have argued Arctic sea ice loss has a pronounced influence on extreme winter weather events at midlatitudes (Francis & Vavrus, 2012; Liu et al., 2012; Mori et al., 2014). The evidence for a causal link between Arctic SIE anomalies and midlatitude weather is not clearly supported by observations and is highly sensitive to the choice of methodology (Barnes, 2013; Barnes & Screen, 2015; McCusker et al., 2016). As summarized in Wallace et al. (2014): *alternative observational analyses and simulations with climate models have not confirmed the hypothesis that Arctic SIE loss exhibits a causal relationship with midlatitude weather.*

The purpose of this paper is to analyze the observed lead/lag relationships between variations in (1) Arctic SIE and (2) Arctic atmospheric temperatures and high-latitude circulation. Previous studies have focused on the linkages between large-scale climate and sea ice anomalies either at the end of summer melt season (e.g., September; Francis et al., 2009; Honda et al., 2009; Koyama et al., 2017; Serreze et al., 2016) or averaged over the entire summer (Kay & Gettelman, 2009; Knudsen et al., 2015). In contrast to those studies, we demonstrate that the continuous (i.e., not reemerging) lagged linkages between sea ice anomalies and high-latitude climate are most robust in association with midsummer (July) SIE. For example, we show that September SIE is only significantly linked to high-latitude climate up to 1 month in advance, whereas midsummer SIE anomalies are significantly linked to high-latitude climate up to three consecutive months in advance. The linkages between midsummer SIE anomalies and high-latitude climate are significantly well in autumn and have potential implications for the prediction of Arctic climate and the interpretation of the climate response to future sea ice loss.

2. Data Sets and Methods

We use three data sources to assess the predictability of high-latitude climate that derives from midsummer Arctic SIE anomalies.

1. *Observations.* Sea ice concentration data and the time series of Arctic-average SIE were obtained from the National Snow and Ice Data Center (Comiso, 2017; Fetterer et al., 2017). Atmospheric variables are based on output from the Interim European Reanalysis product (Dee et al., 2011). Observations are analyzed in monthly-mean form over the period 1979–2016 with the exception of Figures S1 and S2 in the supporting information, which are based on daily-mean data.
2. *CMIP5 output.* Results from observations are compared with analogous results calculated for simulated SIC and surface air temperature output from the fifth phase of the Coupled Model Intercomparison Project (CMIP5). The CMIP5 output is based on historical simulations (1900–2005) from 28 coupled models (see Table S1 in the supporting information). The CMIP5 output is analyzed in monthly-mean form over the period 1900–2005.
3. *APPOSITE output.* The predictability inferred from the observational analyses is also explored in output from the Arctic Predictability and Prediction on Seasonal to Interannual Time scales (APPOSITE) project (Day et al., 2015). The APPOSITE model experiments are specifically designed to assess the predictability of Arctic climate. Details of the experiments are provided in Day et al. (2015). In short, the experiments are conducted as follows. Long (multiple centuries) control experiments are performed with a series of coupled ocean-atmosphere-sea ice general circulation models (GCMs). The control simulations are then used as a baseline for assessing predictability in a series of initial-value experiments run on the same models (i.e., the model predictions are verified against the respective model controls, the so-called *perfect model* approach). The prediction experiments have lengths between 8 and 12 years (the exact number varies from model to model), and start years for ensemble predictions are chosen from the control simulation. The predictability of various climate variables is then assessed using anomaly correlation coefficients (for details refer to Tietsche et al., 2014), where values exceeding 0.6 are considered as providing potential positive skill. Here four coupled atmosphere-ocean-sea ice GCMs were chosen for

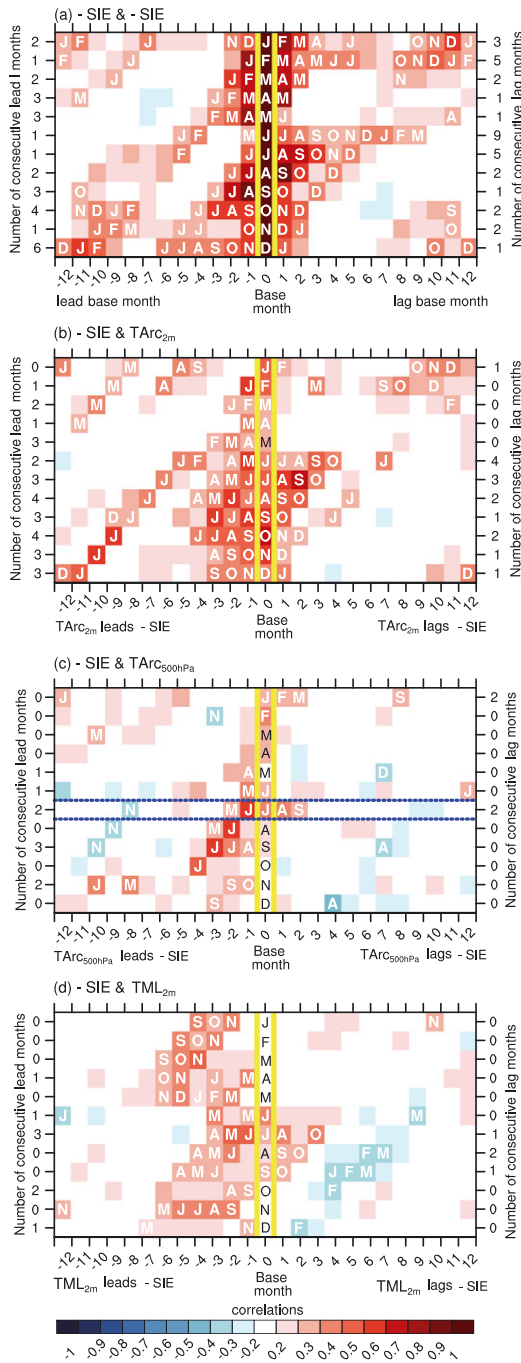


Figure 1. Monthly lead/lag correlation coefficients between Arctic (a) SIE and SIE (i.e., the autocorrelation of SIE), (b) SIE and T_{Arc2m} , (c) SIE and $T_{Arc500hPa}$, and (d) SIE and T_{ML2m} . $T_{Arc500hPa}$ is area-averaged 500-hPa temperature over the Arctic (65–90°N), and T_{ML2m} is defined as midlatitude land-mean 2-m temperature averaged over 40–70°N. Numbers on the ordinate axis denote the number of consecutive months that a significant lead/lag correlation occurs for each base month; negative/positive values on the abscissa denote the lead/lag months for the base month. Correlations that are significant at the 95% confidence level are indicated by including the white letter of the lead/lag month. The SIE base index is inverted (i.e., the correlation coefficients correspond to temperature anomalies associated with anomalously low Arctic SIE). All data are deseasonalized and detrended. SIE = sea ice extent.

analysis based on the criteria that (1) output is provided for the required variables for our analyses (notably, surface air temperature) and (2) the experiments were integrated for at least 200 years. The models chosen for analyses are the MPI-ESM, HadGEM1–2, ECHAM6-FESOM, and GFDL-CM3 (see Tietsche et al., 2014 for details). Lead/lag correlations and linear regressions are based on deseasonalized and linearly detrended versions of the time series. Detrending ensures that shared trends in the time series (e.g., due to the global warming of the past few decades) do not influence the statistical results. Detrending using a quadratic approximation gives similar results (not shown). The basis for the regressions is a standardized, inverted index of SIE averaged over the Arctic basin, referred to herein as the Arctic SIE time series. Note that positive values of the inverted Arctic SIE time series indicate low SIE, and vice versa. Statistical significance is estimated using a two-tailed test of Student’s *t* distribution after accounting for the effects of persistence in the time series on sample size.

3. Results

As noted in section 1, the persistence of Arctic sea ice has been explored in numerous previous studies during various times of the year (e.g., Blanchard-Wrigglesworth, Armour, et al., 2011; Deser et al., 2010; Honda et al., 2009; Liu et al., 2012; Rigor & Wallace, 2004). Figure 1a explores the autocorrelation of the Arctic SIE time series associated with all possible base months. The results confirm numerous key aspects of sea ice variability highlighted in previous studies (e.g., Blanchard-Wrigglesworth, Armour, et al., 2011) and also provide several novel findings. For instance, the results make clear that SIE anomalies exhibit continuous significant memory at positive lags up to 9 months into the future from midsummer, which is notably longer than the persistence indicated in Blanchard-Wrigglesworth, Armour, et al. (2011). The results also confirm that SIE anomalies exhibit reemergence at least 12 months into the future during the growth season months of January and February but reveal that such reemergence is much less clear in association with March and April SIE anomalies.

The bottom three panels in Figure 1 show the corresponding lead/lag correlation coefficients between inverted values of Arctic SIE and (b) Arctic-mean 2-m temperature (T_{Arc2m}), (c) Arctic-mean 500-hPa air temperature ($T_{Arc500hPa}$) averaged over 65–90°N, and (d) midlatitude land-mean 2-m temperature averaged over 40–70°N (T_{ML2m}). As expected, periods of anomalously low SIE are preceded by anomalously warm surface conditions during most times of year, consistent with forcing of the sea ice field by the anomalous fluxes of sensible and latent heat from the atmosphere to the ocean (Ding et al., 2017; Maykut, 1982; Mortin et al., 2016). For example, negative Arctic SIE anomalies during the months May to December are significantly (and continuously) linked to warm conditions during the previous 2–4 months. Interestingly, SIE anomalies in the cold season months of January and February are not strongly linked to preceding atmospheric temperatures (Figure 1b), presumably since the Arctic is largely ice covered in January and February regardless of the temperature anomalies in previous months. The inferred forcing of Arctic SIE by atmospheric temperatures is less clear in results based on Arctic-mean 500-hPa temperatures but is readily apparent in midlatitude land-mean surface temperature, that is, anomalously warm

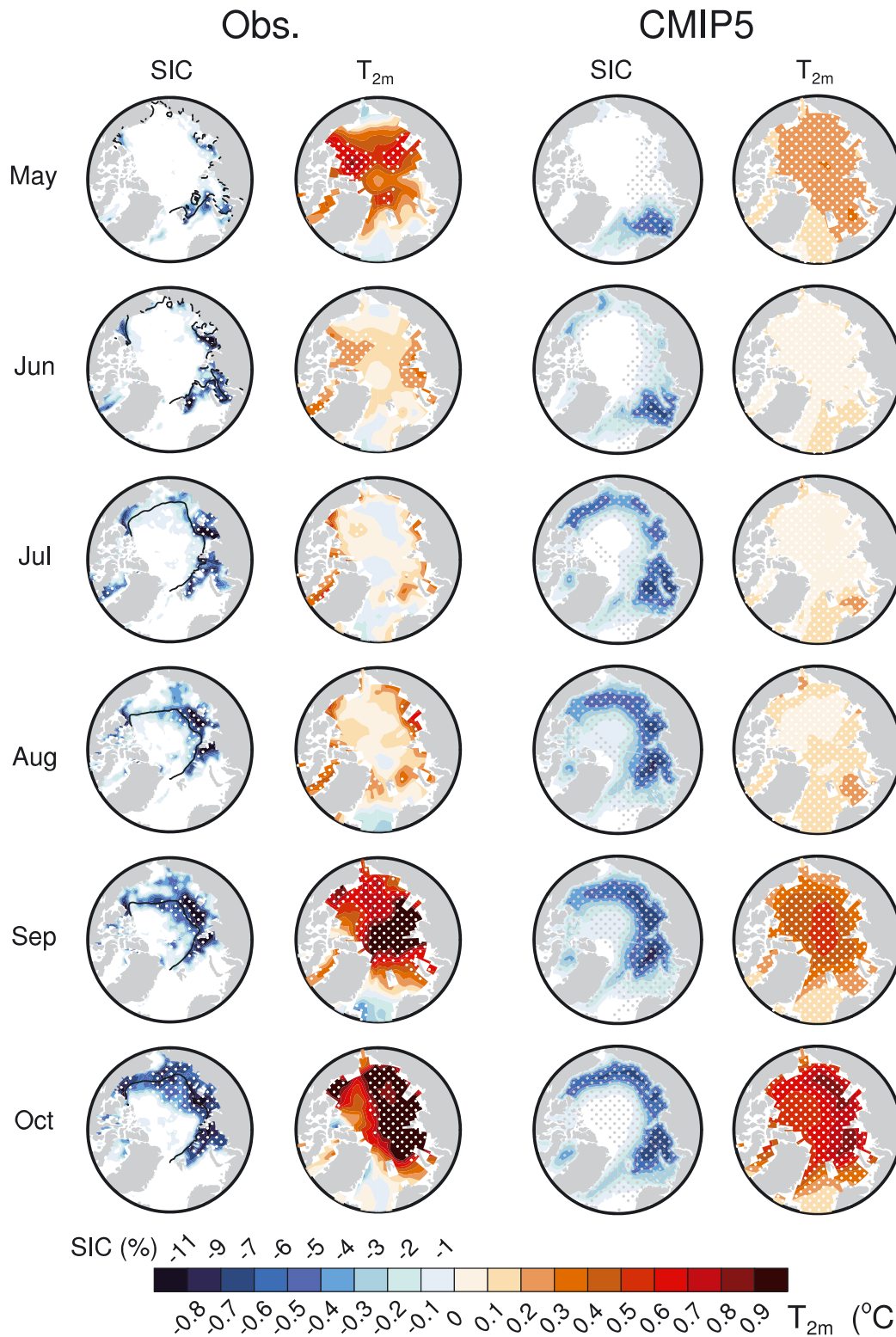


Figure 2. (first column) Sea ice concentration (SIC; in %) averaged over the months regressed onto the inverted time series of July-mean Arctic SIE (i.e., regression coefficients are shown in physical units per standard deviation of Arctic SIE reduction); the black contours indicate the isoline of 70% in the climatology SIC. (second column) As in the first column but for the surface air temperature at 2 m (T_{2m} ; in K) regressed onto the inverted time series of July-mean Arctic SIE. Results are calculated for the period 1979–2016. Dots indicate regions of regression coefficients that are significant at the 95% confidence level. (third and fourth columns) Same as the first and second columns, respectively, but based on results averaged over coupled climate models from the historical CMIP5 simulations (the 28 simulations are listed in Table S1 in the supporting information). SIE = sea ice extent; CMIP5 = fifth phase of the Coupled Model Intercomparison Project.

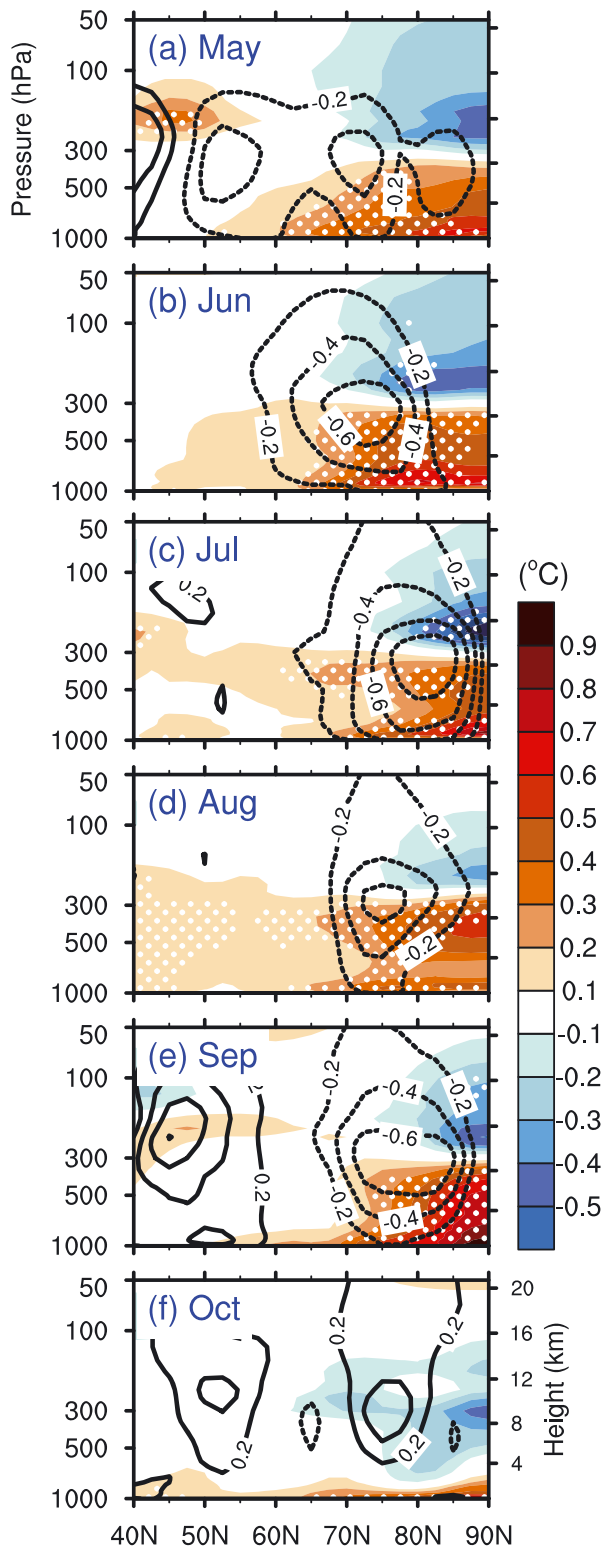


Figure 3. Zonally averaged temperature (T ; shading; in degree Celsius) and zonal wind (u ; contours; in m/s) averaged over the months indicated regressed onto the inverted time series of July-mean Arctic SIE. Results are calculated for the period 1979–2016. White dots indicate regions where the temperature anomalies are statistically significant at the 95% confidence level. SIE = sea ice extent.

conditions over midlatitudes of the Northern Hemisphere (NH) land masses precede periods of anomalously low Arctic SIE (recall that the data are detrended, so the results do not simply reflect shared trends in NH land temperatures and Arctic SIE).

The most interesting result in Figures 1b–1d is that SIE anomalies not only lag significant anomalies in atmospheric temperatures but also lead them (i.e., see results at positive lag in Figures 1b and 1d). Summer SIE anomalies exhibit robust and persistent correlations with Arctic surface temperatures at positive lags of up to 2–4 months (Figure 1b). The persistence of the positive correlations associated with summer SIE anomalies is longer than that associated with September SIE, which is the basis for exploring lead/lag relationships between summer SIE anomalies and Arctic climate in numerous previous studies (e.g., Francis et al., 2009; Koyama et al., 2017). Importantly, the correlations between July Arctic SIE and September temperature anomalies exceed the autocorrelation of the temperature field (see Figure S1). Hence, the lag correlations between July SIE and September temperature anomalies derive in part from the addition of information from the sea ice field.

Interestingly, the temperature anomalies linked to midsummer SIE are largest at the surface (Figure 1b) and also extend to the middle troposphere (Figure 1c) and midlatitude land-mean surface temperatures (Figure 1d). The negative correlations between the inverted Arctic SIE time series in September and midlatitude land temperature in winter are interesting and consistent with some previous findings (e.g., Honda et al., 2009; Liu et al., 2012), but here we focus on the persistence of the warming at shorter time lags.

The persistence of midsummer Arctic sea ice anomalies is explored further in Figure 2, which shows the lead/lag regressions between inverted values of July-mean Arctic SIE and (first column) monthly-mean values of SIC from May to October. Note that the regression coefficients are in physical units per standard deviation of the inverted Arctic SIE time series. During the early-summer and midsummer months (May to July), years with anomalously low Arctic-mean SIE are preceded by anomalously low SIC anomalies over the Barents, Kara, and Laptev seas. The regions of statistically significantly low SIC grow through summer and expand dramatically into the Chukchi and Beaufort seas in August, September, and October. Note that the enlarging of significant SIC anomalies coincides with the retreat of the seasonal-mean sea ice cover (black contour). That is, the sea ice anomalies exhibit most memory along the edge of the ice pack where the ice is relatively thin.

The linkages between midsummer Arctic SIE anomalies and surface air temperature (T_{2m} ; Figure 2, second column) peak during the preceding spring and following fall months. As noted above, the anomalies during spring indicate forcing of Arctic SIE by atmospheric temperatures, but the widespread significant anomalies during autumn indicate a robust link between midsummer SIE anomalies and Arctic surface temperatures during the autumn season. Low SIE conditions during summer 2007 were followed by similarly warm conditions over the Arctic (Orsolini et al., 2012).

The above observed results are readily reproduced in historical simulations from the CMIP5 archive (Figure 2, third and fourth columns), which shows the same variables as the first and second columns in Figure 2, but averaged over the 28 coupled models listed in Table S1 in the

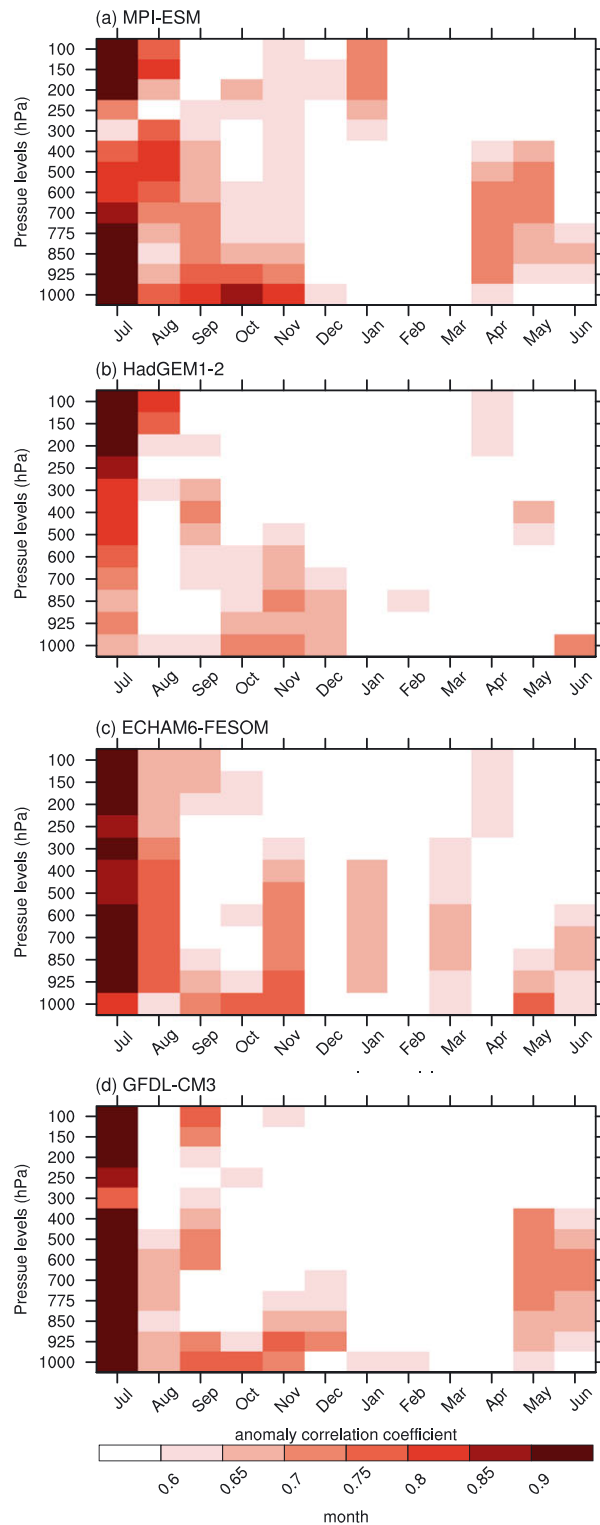


Figure 4. The anomaly correlation coefficient for Arctic-mean (north of 65°N) air temperature derived from four models from the APPOSITE project. Shaded values indicate levels and months where coupled GCMs initialized on 1 July exhibit significant predictive skill. The models are (a) MPI-ESM, (b) HadGEM1-2, (c) ECHAM6-FESOM, and (d) GFDL-CM3. GCMs = general circulation models; APPOSITE = Arctic Predictability and Prediction on Seasonal to Interannual Time scales.

supporting information. The spatial patterns of the SIC and surface temperature anomalies bear strong resemblance to the observations at all lags: periods of low July Arctic-mean SIE are followed by significantly low SIC stretching along the Siberian and Alaskan coasts of Arctic (third column) and by significant surface warming throughout the Arctic that has largest amplitude during the autumn months (Figure 2, fourth column). Note that the regressions between July SIE and T_{2m} are comparably significant during September and October but have larger amplitude in October since the variance of the temperature field is larger at that time.

Figure 3 shows meridional cross sections of monthly-mean, zonally averaged atmospheric temperatures and zonal winds regressed onto standardized and inverted values of the July Arctic-mean SIE time series (i.e., the same index used to generate the first two columns in Figure 2). Figure S2 shows a time/height plot of correlations between Arctic-mean atmospheric temperatures and the same index but for daily-mean data. As discussed above in the context of Figure 1b, the results at negative lag (i.e., May–June) are consistent with forcing of the sea ice field by atmospheric temperature and circulation (e.g., Blanchard-Wrigglesworth, Armour, et al., 2011; Rigor & Wallace, 2004). Midsummers characterized by low sea ice conditions are preceded by positive tropospheric temperature anomalies across high latitudes from May to June (Figures 3a and 3b and S2). In July and August, robust warm anomalies extend from the surface into the free troposphere (Figures 3c and 3d and S2). Note that the Arctic temperature anomalies associated with July Arctic SIE are significant in October when they are confined to the surface (Figures 3f and S2). Consistent with the thermal wind relation, the positive temperature anomalies during August and September are associated with easterly wind anomalies of ~0.4–0.8 m/s centered at ~70°N (Figures 3d and 3e, contours).

Previous studies have emphasized the predictability of NH climate that derives from September SIE anomalies (e.g., Francis et al., 2009; Koyama et al., 2017). An important distinction between our study and previous work is that the inferred predictability from midsummer SIE is ~2–3 months (Figures 1–3), whereas that associated with September SIE anomalies is only ~1 month, that is, September SIE anomalies are only followed by significant Arctic surface temperature anomalies at 1 month into the future (Figures 1b and S3).

Together, the results in Figures 1–3 indicate that the linkages between midsummer SIE anomalies and Arctic temperatures during autumn are a robust feature of Arctic climate. The findings suggest that SIE anomalies during midsummer provide predictive skill of high-latitude climate during the following autumn months, and that the skill derives from the influence of persistent sea ice anomalies on the overlying atmosphere. The results are physically consistent with enhanced sensible and latent fluxes of heat into the atmosphere associated with persistent anomalies in the sea ice field. The results are also reproducible in the historical simulations in the CMIP5 archive and in initial value experiments run under the auspices of the APPOSITE project.

Figure 4 shows the predictability of Arctic-mean temperature derived from four coupled atmosphere-ocean-sea ice GCMs initialized on 1 July from the APPOSITE archive (see section 2 and Day et al., 2015 for details).

As shown in the figure, Arctic-mean air temperature exhibits persistent potential predictability from midsummer through autumn, and the potential predictability of Arctic middle/upper tropospheric air temperature is higher in August and September than it is in October. Though the source of predictability in APPOSITE cannot be uniquely attributed to sea ice anomalies, the predictive skill indicated by the coupled GCMs from the APPOSITE project is consistent with our interpretation that midsummer conditions over the Arctic lead to predictive skill over the Arctic basin well into the autumn months. In fact, as indicated in Day et al. (2014) *initializing predictions of extent and volume in July has strong advantages for the prediction of the September minimum*. Note that similar predictive skill is not found for results initialized on 1 January (Figure S4).

4. Conclusions

Previous work has explored the potential impact of summertime Arctic SIE on the large-scale circulation but has focused primarily on sea ice anomalies at the *end* of summer melt season (September; Francis et al., 2009; Honda et al., 2009; Koyama et al., 2017; Serreze et al., 2016) or sea ice melt averaged over the entire summer (Kay & Gettelman, 2009; Knudsen et al., 2015). Here we have demonstrated that midsummer Arctic SIE anomalies exhibit pronounced potential predictability (at lags of 2–3 months) of the atmospheric circulation and temperature at high latitudes. The skill inferred from midsummer conditions (Figure 3) is notably longer than that inferred from late summer conditions (Figure S3).

The intrinsic time scale of large-scale atmospheric extratropical variability is only ~10 days (forcing from the tropics, e.g., ENSO, can contribute to autocorrelation of the extratropical circulation but is not significantly correlated with the Arctic-mean surface temperature time series used here). Hence, the linkages shown here suggest a measure of predictability of Arctic climate at lead times of several months. Midsummers characterized by low sea ice conditions are followed by positive temperature anomalies throughout the Arctic that persist in September into the free atmosphere and into October at the surface (Figures 1–3 and S2). The warming of the Arctic atmosphere during August to September is accompanied by robust changes in the zonal wind encircling the Arctic basin (Figure 3). Importantly, the time/space evolution of the linkages between midsummer Arctic SIE and Arctic surface temperature is reproducible in historical runs with coupled climate models (Figure 2), and the inferred predictive skill is mirrored in coupled climate model experiments initialized on 1 July from the APPOSITE project (Figure 4). That the linkages between SIE anomalies in midsummer and surface temperatures during autumn extend to midlatitude land-mean temperature (Figures 1d and S5) suggests that the anomalies in surface heat fluxes associated with Arctic SIE anomalies are sufficiently large to noticeably project onto the midlatitude land-mean energy budget.

Arctic SIE shows the most dominant melt in summer due to larger energy uptake in this season (e.g., Knudsen et al., 2015; Mortin et al., 2016; Stroeve et al., 2014). In these months, the sea ice and ocean systems receive large input of heat from above, and differences in absorption rates lead to anomalous oceanic heat storage that can be returned to the atmosphere in autumn and winter and make an imprint on the climate system. Hence, the seasonal relationships between midsummer SIE and autumn Arctic climate highlighted here likely derive from (1) the anomalous storage of heat in the Arctic Ocean during periods of low midsummer SIE and (2) the delay in the formation of sea ice during the following months, which should increase the anomalous fluxes of heat into the Arctic atmosphere due to the increased areas of open ocean. The mechanisms and implications of the linkages shown here for Arctic climate are currently under investigation in numerical hindcast experiments in a companion study.

References

- Alexander, M. A., Bhatt, U. S., Walsh, J. E., Timlin, M. S., Miller, J. S., & Scott, J. D. (2004). The atmospheric response to realistic Arctic sea ice anomalies in an AGCM during winter. *Journal of Climate*, 17(5), 890–905. [https://doi.org/10.1175/1520-0442\(2004\)017<0890:TARTRA>2.0.CO;2](https://doi.org/10.1175/1520-0442(2004)017<0890:TARTRA>2.0.CO;2)
- Årthun, M., Eldevik, T., Viste, E., Drange, H., Furevik, T., Johnson, H. L., & Keenlyside, N. S. (2017). Skillful prediction of northern climate provided by the ocean. *Nature Communications*, 8, 15875. <https://doi.org/10.1038/ncomms15875>
- Barnes, E. A., & Screen, J. A. (2015). The impact of Arctic warming on the midlatitude jet-stream: Can it? Has it? Will it? *Wiley Interdisciplinary Reviews: Climate Change*, 6(3), 277–286.
- Barnes, E. A. (2013). Revisiting the evidence linking Arctic amplification to extreme weather in midlatitudes. *Geophysical Research Letters*, 40, 4734–4739. <https://doi.org/10.1002/grl.50880>
- Barnett, D. G. (1980). *A long-range ice forecasting method for the north coast of Alaska*. Seattle, WA: University of Washington Press.

Acknowledgments

We thank three anonymous reviewers for valuable comments that helped improve the manuscript. Atmospheric ERA-Interim data were provided by the European Centre for Medium-Range Weather Forecasts (ECMWF; <https://www.ecmwf.int/en/research/climate-reanalysis/era-interim>). Sea ice data were provided by NSIDC (https://nsidc.org/data/seaice_index/). CMIP5 historical simulations are available at website http://www.ipcc-data.org/sim/gcm_monthly/AR5/Reference-Archive.html. Data sets of APPOSITE are available at website <http://catalogue.ceda.ac.uk/uuid/d330c7873c3f4880893bde547bea20>. The study has been supported by the Research Council of Norway, through the BlueArc project (207650), and the German Research Foundation through the Transregional Collaborative Research Center (TR 172) **Arctic Amplification: Climate Relevant Atmospheric and Surface Processes, and Feedback Mechanisms (AC³)**, and the National Natural Science Foundation of China (41505073). S. H. and T. F. are funded by a grant from the Norwegian Ministry of Education and Research, and D. W. J. T. is funded by the Climate and Large-Scale Dynamics program from National Science Foundation.

- Bhatt, U. S., Alexander, M. A., Deser, C., Walsh, J. E., Miller, J. S., Timlin, M., et al. (2008). The atmospheric response to realistic reduced summer Arctic sea ice anomalies. Arctic sea ice decline: Observations, projections, mechanisms, and implications. *Geophysical Monograph*, 180, 91–110.
- Blanchard-Wrigglesworth, E., Armour, K. C., Bitz, C. M., & DeWeaver, E. (2011). Persistence and inherent predictability of Arctic sea ice in a GCM ensemble and observations. *Journal of Climate*, 24(1), 231–250. <https://doi.org/10.1175/2010JCLI3775.1>
- Blanchard-Wrigglesworth, E., Bitz, C., & Holland, M. (2011). Influence of initial conditions and climate forcing on predicting Arctic sea ice. *Geophysical Research Letters*, 38, L18503. <https://doi.org/10.1029/2011GL048807>
- Blüthgen, J., Gerdes, R., & Werner, M. (2012). Atmospheric response to the extreme Arctic sea ice conditions in 2007. *Geophysical Research Letters*, 39, L02707. <https://doi.org/10.1029/2011GL050486>
- Budyko, M. (1969). The effect of solar radiation variations on the climate of the Earth. *Tellus*, 21, 611–619.
- Chevallier, M., Salas y Mélia, D., Voldoire, A., Déqué, M., & Garric, G. (2013). Seasonal forecasts of the pan-Arctic sea ice extent using a GCM-based seasonal prediction system. *Journal of Climate*, 26(16), 6092–6104. <https://doi.org/10.1175/JCLI-D-12-00612.1>
- Comiso, J. C. (2017). *Bootstrap sea ice concentrations from Nimbus-7 SMMR and DMSP SSM/I-SSMIS, version 3. [indicate subset used]*. Boulder, Colorado USA: NASA National Snow and Ice Data Center Distributed Active Archive Center. <https://doi.org/10.5067/7Q8HCCWS4I0R>
- Cvijanovic, I., Santer, B. D., Bonfils, C., Lucas, D. D., Chiang, J. C. H., & Zimmerman, S. (2017). Future loss of Arctic sea-ice cover could drive a substantial decrease in California's rainfall. *Nature Communications*, 8(1), 1947. <https://doi.org/10.1038/s41467-017-01907-4>
- Day, J., Hawkins, E., & Tietsche, S. (2015). Collection of multi-model data from the Arctic predictability and prediction on seasonal-to-interannual time-scales (APPOSITE) project. NCAS British Atmospheric Data Centre, 06 September 2015. <https://doi.org/10.5285/45814db8-56cd-44f2-b3a4-92e41eaaff3f>
- Day, J., Tietsche, S., & Hawkins, E. (2014). Pan-Arctic and regional sea ice predictability: Initialization month dependence. *Journal of Climate*, 27(12), 4371–4390. <https://doi.org/10.1175/JCLI-D-13-00614.1>
- Dee, D., Uppala, S., Simmons, A., Berrisford, P., Poli, P., Kobayashi, S., et al. (2011). The ERA-Interim reanalysis: Configuration and performance of the data assimilation system. *Quarterly Journal of the Royal Meteorological Society*, 137(656), 553–597. <https://doi.org/10.1002/qj.828>
- Deser, C., Magnusdottir, G., Saravanan, R., & Phillips, A. (2004). The effects of North Atlantic SST and sea-ice anomalies on the winter circulation in CCM3, Part II: Direct and indirect components of the response. *Journal of Climate*, 17(5), 877–889. [https://doi.org/10.1175/1520-0442\(2004\)017<0877:TEONAS>2.0.CO;2](https://doi.org/10.1175/1520-0442(2004)017<0877:TEONAS>2.0.CO;2)
- Deser, C., Tomas, R., Alexander, M., & Lawrence, D. (2010). The seasonal atmospheric response to projected Arctic sea ice loss in the late twenty-first century. *Journal of Climate*, 23(2), 333–351. <https://doi.org/10.1175/2009JCLI3053.1>
- Ding, Q., Schweiger, A., L'Heureux, M., Battisti, D. S., Po-Chedley, S., Johnson, N. C., et al. (2017). Influence of high-latitude atmospheric circulation changes on summertime Arctic sea ice. *Nature Climate Change*, 7(4), 289–295. <https://doi.org/10.1038/nclimate3241>
- Drobot, S. D. (2007). Using remote sensing data to develop seasonal outlooks for Arctic regional sea-ice minimum extent. *Remote Sensing of Environment*, 111(2-3), 136–147. <https://doi.org/10.1016/j.rse.2007.03.024>
- Fetterer, F., Knowles, K., Meier, W., Savoie, M., & Windnagel, A. K. (2017). Updated daily. Sea ice index, version 3. [indicate subset used]. Boulder, Colorado USA. NSIDC: National Snow and Ice Data Center. <https://doi.org/10.7265/N5K072F8>
- Francis, J., & Vavrus, S. (2012). Evidence linking Arctic amplification to extreme weather in mid-latitudes. *Geophysical Research Letters*, 39, L06801. <https://doi.org/10.1029/2012GL051000>
- Francis, J. A., Chan, W., Leathers, D. J., Miller, J. R., & Veron, D. E. (2009). Winter Northern Hemisphere weather patterns remember summer Arctic sea-ice extent. *Geophysical Research Letters*, 36, L07503. <https://doi.org/10.1029/2009GL037274>
- Frankignoul, C., Sennéchal, N., & Cauchy, P. (2014). Observed atmospheric response to cold season sea ice variability in the Arctic. *Journal of Climate*, 27(3), 1243–1254. <https://doi.org/10.1175/JCLI-D-13-00189.1>
- Gao, Y., Sun, J., Li, F., He, S., Sandven, S., Yan, Q., et al. (2015). Arctic sea ice and Eurasian climate: A review. *Advances in Atmospheric Sciences*, 32(1), 92–114. <https://doi.org/10.1007/s00376-014-0009-6>
- Herman, G. T., & Johnson, W. T. (1978). The sensitivity of the general circulation of Arctic sea ice boundaries: A numerical experiment. *Monthly Weather Review*, 106(12), 1649–1664. [https://doi.org/10.1175/1520-0493\(1978\)106<1649:TSOTGC>2.0.CO;2](https://doi.org/10.1175/1520-0493(1978)106<1649:TSOTGC>2.0.CO;2)
- Holland, M. M., Bailey, D. A., & Vavrus, S. (2011). Inherent sea ice predictability in the rapidly changing Arctic environment of the Community Climate System Model, version 3. *Climate Dynamics*, 36(7–8), 1239–1253. <https://doi.org/10.1007/s00382-010-0792-4>
- Honda, M., Inoue, J., & Yamane, S. (2009). Influence of low Arctic sea-ice minima on anomalously cold Eurasian winters. *Geophysical Research Letters*, 36, L08707. <https://doi.org/10.1029/2008GL037079>
- Kay, J. E., & Gettelman, A. (2009). Cloud influence on and response to seasonal Arctic sea ice loss. *Journal of Geophysical Research*, 114, D18204. <https://doi.org/10.1029/2009JD011773>
- Kirtma, B., Power, S. B., Adedoyin, J. A., Boer, G. J., Bojariu, R., Camilloni, I., et al. (2013). Near-term climate change: Projections and predictability. In *Climate change 2013: The Physical Science Basis. Contribution of Working Group I to the Fifth Assessment Report of the Intergovernmental Panel on Climate Change* (pp. 953–1028). Cambridge, United Kingdom and New York, NY, USA: Cambridge University Press. <https://doi.org/10.1017/CBO9781107415324.023>
- Knudsen, E. M., Orsolini, Y. J., Furevik, T., & Hodges, K. I. (2015). Observed anomalous atmospheric patterns in summers of unusual Arctic sea ice melt. *Journal of Geophysical Research: Atmospheres*, 120, 2595–2611. <https://doi.org/10.1002/2014JD022608>
- Koyama, T., Stroeve, J., Cassano, J., & Crawford, A. (2017). Sea ice loss and Arctic cyclone activity from 1979 to 2014. *Journal of Climate*, 30(12), 4735–4754. <https://doi.org/10.1175/JCLI-D-16-0542.1>
- Lindsay, R., Zhang, J., Schweiger, A., & Steele, M. (2008). Seasonal predictions of ice extent in the Arctic Ocean. *Journal of Geophysical Research*, 113, C02023. <https://doi.org/10.1029/2007JC004259>
- Liu, J., Curry, J. A., Wang, H., Song, M., & Horton, R. M. (2012). Impact of declining Arctic sea ice on winter snowfall. *Proceedings of the National Academy of Sciences*, 109, 6781–6783.
- Maykut, G. A. (1982). Large-scale heat exchange and ice production in the central Arctic. *Journal of Geophysical Research*, 87(C10), 7971–7984. <https://doi.org/10.1029/JC087iC10p07971>
- McCusker, K. E., Fyfe, J. C., & Sigmond, M. (2016). Twenty-five winters of unexpected Eurasian cooling unlikely due to Arctic sea-ice loss. *Nature Geoscience*, 9(11), 838–842. <https://doi.org/10.1038/ngeo2820>
- Mori, M., Watanabe, M., Shiogama, H., Inoue, J., & Kimoto, M. (2014). Robust Arctic sea-ice influence on the frequent Eurasian cold winters in past decades. *Nature Geoscience*, 7(12), 869–873. <https://doi.org/10.1038/ngeo2277>
- Mortin, J., Svensson, G., Graverson, R. G., Kapsch, M. L., Stroeve, J. C., & Boisvert, L. N. (2016). Melt onset over Arctic sea ice controlled by atmospheric moisture transport. *Geophysical Research Letters*, 43, 6636–6642. <https://doi.org/10.1002/2016GL069330>
- Orsolini, Y. J., Senan, R., Benestad, R. E., & Melsom, A. (2012). Autumn atmospheric response to the 2007 low Arctic sea ice extent in coupled ocean-atmosphere hindcasts. *Climate Dynamics*, 38(11–12), 2437–2448. <https://doi.org/10.1007/s00382-011-1169-z>

- Petrie, R. E., Shaffrey, L. C., & Sutton, R. T. (2015). Atmospheric response in summer linked to recent Arctic sea ice loss. *Quarterly Journal of the Royal Meteorological Society*, *141*(691), 2070–2076. <https://doi.org/10.1002/qj.2502>
- Rigor, I. G., & Wallace, J. M. (2004). Variations in the age of Arctic sea-ice and summer sea-ice extent. *Geophysical Research Letters*, *31*, L09704. <https://doi.org/10.1029/2004GL019492>
- Screen, J. A., Deser, C., Simmonds, I., & Tomas, R. (2014). Atmospheric impacts of Arctic sea-ice loss, 1979–2009: Separating forced change from atmospheric internal variability. *Climate Dynamics*, *43*(1–2), 333–344. <https://doi.org/10.1007/s00382-013-1830-9>
- Screen, J. A., Simmonds, I., Deser, C., & Tomas, R. (2013). The atmospheric response to three decades of observed Arctic sea ice loss. *Journal of Climate*, *26*(4), 1230–1248. <https://doi.org/10.1175/JCLI-D-12-00063.1>
- Serreze, M. C., & Barry, R. G. (2011). Processes and impacts of Arctic amplification: A research synthesis. *Global and Planetary Change*, *77*(1–2), 85–96. <https://doi.org/10.1016/j.gloplacha.2011.03.004>
- Serreze, M. C., Holland, M. M., & Stroeve, J. (2007). Perspectives on the Arctic's shrinking sea-ice cover. *Science*, *315*(5818), 1533–1536. <https://doi.org/10.1126/science.1139426>
- Serreze, M. C., Stroeve, J., Barrett, A. P., & Boisvert, L. N. (2016). Summer atmospheric circulation anomalies over the Arctic Ocean and their influences on September sea ice extent: A cautionary tale. *Journal of Geophysical Research: Atmospheres*, *121*, 11,463–11,485. <https://doi.org/10.1002/2016JD025161>
- Sigmond, M., Fyfe, J., Flato, G., Kharin, V., & Merryfield, W. (2013). Seasonal forecast skill of Arctic sea ice area in a dynamical forecast system. *Geophysical Research Letters*, *40*, 529–534. <https://doi.org/10.1002/grl.50129>
- Stroeve, J., Crawford, A. D., & Stammerjohn, S. (2016). Using timing of ice retreat to predict timing of fall freeze-up in the Arctic. *Geophysical Research Letters*, *43*, 6332–6340. <https://doi.org/10.1002/2016GL069314>
- Stroeve, J., Holland, M. M., Meier, W., Scambos, T., & Serreze, M. (2007). Arctic sea ice decline: Faster than forecast. *Geophysical Research Letters*, *34*, L09501. <https://doi.org/10.1029/2007GL029703>
- Stroeve, J., Markus, T., Boisvert, L., Miller, J., & Barrett, A. (2014). Changes in Arctic melt season and implications for sea ice loss. *Geophysical Research Letters*, *41*, 1216–1225. <https://doi.org/10.1002/2013GL058951>
- Tietsche, S., Day, J. J., Guemas, V., Hurlin, W. J., Keeley, S. P. E., Matei, D., et al. (2014). Seasonal to interannual Arctic sea ice predictability in current global climate models. *Geophysical Research Letters*, *41*, 1035–1043. <https://doi.org/10.1002/2013GL058755>
- Wallace, J. M., Held, I. M., Thompson, D. W., Trenberth, K. E., & Walsh, J. E. (2014). Global warming and winter weather. *Science*, *343*(6172), 729–730. <https://doi.org/10.1126/science.343.6172.729>
- Walsh, J. E. (1980). *Empirical orthogonal functions and the statistical predictability of sea ice extent, sea ice processes and models* (pp. 373–384). Seattle: University of Washington Press.
- Walsh, J. E., & Johnson, C. M. (1979). An analysis of Arctic sea ice fluctuations, 1953–77. *Journal of Physical Oceanography*, *9*(3), 580–591. [https://doi.org/10.1175/1520-0485\(1979\)009<0580:AAOASI>2.0.CO;2](https://doi.org/10.1175/1520-0485(1979)009<0580:AAOASI>2.0.CO;2)
- Wang, W., Chen, M., & Kumar, A. (2013). Seasonal prediction of Arctic sea ice extent from a coupled dynamical forecast system. *Monthly Weather Review*, *141*(4), 1375–1394. <https://doi.org/10.1175/MWR-D-12-00057.1>
- Yeager, S. G., Karspeck, A. R., & Danabasoglu, G. (2015). Predicted slowdown in the rate of Atlantic sea ice loss. *Geophysical Research Letters*, *42*, 10,704–10,713. <https://doi.org/10.1002/2015GL065364>